ELSEVIER

Contents lists available at ScienceDirect

Journal of Colloid And Interface Science

journal homepage: www.elsevier.com/locate/jcis



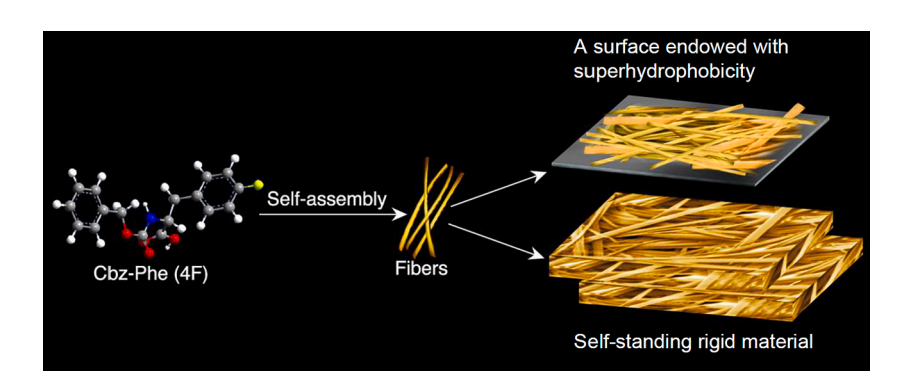


A self-standing superhydrophobic material formed by the self-assembly of an individual amino acid

Tan Hu^a, Zhuo Zhang b,c,*, Meital Reches a,*

- ^a Institute of Chemistry and The Center for Nanoscience and Nanotechnology, The Hebrew University of Jerusalem, Jerusalem 91904, Israel
- ^b College of Food Science and Technology, Huazhong Agricultural University, Wuhan 430070, China
- c Key Laboratory of Environment Correlative Dietology (Huazhong Agricultural University), Ministry of Education, Wuhan 430070, China

GRAPHICAL ABSTRACT



ARTICLE INFO

Keywords:
Amino acids
Self-assembly
Superhydrophobic material
Molecular dynamics simulations
Mechanical properties

ABSTRACT

Hypothesis: There is a growing interest in designing superhydrophobic materials for many applications including self-clean surfaces, separation systems, and antifouling solutions. Peptides and amino acids offer attractive building blocks for these materials since they are biocompatible and biodegradable and can self-assemble into complex ordered structures.

Experiments and Simulations: We designed a self-standing superhydrophobic material through the self-assembly of an individual functionalized aromatic amino acid, Cbz-Phe(4F). The self-assembly of Cbz-Phe(4F) was investigated by experimental and computational methods. Moreover, when drop-casted three times on a solid support, it formed a self-standing superhydrophobic material. The mechanical properties and chemical stability of this self-standing superhydrophobic material were demonstrated.

Findings: The designed Cbz-Phe(4F) self-assembled into fibrous structures in solution. Molecular dynamics (MD) simulations revealed that the fibrous backbone of Cbz-Phe(4F) aggregations was stabilized through hydrogen bonds, whereas the isotropic growth of the aggregates was driven by hydrophobic interactions. Importantly, when drop-casted three times on a solid support, it formed a self-standing superhydrophobic material. Moreover, this material had a high mechanical strength, with a Young's modulus of 53 GPa, resistance to enzymatic

E-mail addresses: zhangzhuo@mail.hzau.edu.cn (Z. Zhang), meital.reches@mail.huji.ac.il (M. Reches).

^{*} Corresponding authors.

degradation, and thermal stability up to $200\,^{\circ}$ C. This study provides a simple strategy to generate smart and functional materials by the simple self-assembly of functional individual amino acids.

1. Introduction

Superhydrophobic materials are needed for generating surfaces with properties of self-cleaning, antifouling, antibacterial, and anti-icing. Other applications for superhydrophobic materials include enhancing molecular sensing, energy harvesting, and oil-water separation systems [1–3]. A superhydrophobic material is defined as a solid having a water contact angle greater than 150° and a low contact angle hysteresis or a low sliding angle of less than 10° . Two main parameters are essential to design a superhydrophobic material: (1) chemistry that results in low surface energy and (2) topography of a hierarchical structure [3-5]. Much progress has been reported in the design and fabrication of superhydrophobic materials [4-6]. Most of these materials have been obtained by using synthetic polymers (i.e., long-chain halogenated carbons) and natural extracts (i.e., natural waves, proteins, and cellulose) [5,7]. It has been acknowledged that synthetic polymers, especially the ones containing halogen atoms, are not eco-friendly [5,8]. In addition, the production of natural extracts involves a complex process with high costs [9,10].

Self-assembled peptides are excellent building blocks for the formation of novel superhydrophobic materials due to their inherent hydrophobicity and hierarchical tructures. Lee et al. reported on the self-assembly of diphenylalanine into vertically aligned peptide nanowires that generated a surface with superhydrophobic properties [11]. However, there are no other reports about superhydrophobic materials through the self-assembly of amino acids and/or peptides. Importantly, the fabrication of superhydrophobic materials requires low manufacturing costs for adequate large-scale production. Therefore, the development of superhydrophobic materials by the self-assembly of the simplest possible building blocks of peptides, i.e., amino acids, is of great interest.

The self-assembly of amino acids and peptides into a variety of artificial nanostructures is considered to be a promising route for fabricating novel functional materials [12–14]. Compared to other biomolecules, amino acids are the simplest building blocks because they are small and do not need synthesis as peptides do. Amino acids can be easily decorated, produced in large-scale quantities, and have inherent biocompatibility. Regarding natural amino acids, only a few amino acids were found to self-assemble [15]. It has been reported that the amino acids L-Phe, L-Trp, L-Tyr, and L-His self-assemble into fibers, nanotubes, and twisted nanosheets, which can be utilized to detect living cells [16,17]. The smallest non-chiral amino acid, L-Gly, was reported to self-assemble into fibrous nanostructures [18].

New approaches to obtain promising materials have been attempted to expand the scope of self-assembled amino acids. One common way is the self-assembly of functionalized amino acids, where functional groups such as 9-fluorenylmethoxycarbonyl (Fmoc), naphthalimide (NI), and lipid chain were introduced into N-termini [15]. The Fmocterminated amino acids (i.e., Fmoc-Phe, Fmoc-Tyr, and Fmoc-Met) exhibit relatively rapid self-assembly kinetics, excellent physical and chemical properties, and have great potential in cell culture, photocatalysis, drug delivery, and antibacterial applications [19]. Hsu et al. reported that NI-terminated amino acid formed a microfiber network hydrogel with aggregation-induced emission properties and strong blue emission under ultraviolet light [20]. Acyl chain-modified amino acids were found to self-assemble into ordered structures that varied from vesicles to helical fibers [21]. Another strategy involves the selfassembly of non-standard amino acids. It was reported that non-coded amino acids such as α , β , and γ -amino acids can self-assemble into different nanoarchitectures [22]. Sarah et al. demonstrated that β-Gly crystals formed by supramolecular packing exhibited a higher

piezoelectric voltage constant than did ceramic and polymeric materials [23]. Importantly, the halogenation of aromatic amino acids is another effective way to increase supramolecular interactions. Metrangolo et al. reported that introducing iodine on the Phe residue results in additional supramolecular interactions stemming from the ability of iodine to behave as a halogen-bond donor as well as a hydrogen and halogen-bond acceptor [24]. Even though there have been many attempts to obtain interesting functional structures by individual amino acids, it remains a challenge to design attractive materials using these building blocks.

Herein, we report the self-assembly of a functionalized amino acid (Cbz-Phe(4F)) into self-standing superhydrophobic materials. Cbz-Phe (4F) can self-assemble into fibrous nanostructures in an aqueous phase. Importantly, Cbz-Phe(4F) formed self-standing materials after having been drop-casted 3 times; it also exhibited superhydrophobic properties (water contact angle $> 150^\circ$) and high stability. Our findings provide a novel strategy for the design and development of attractive superhydrophobic materials using simple self-assembling amino acids.

2. Materials and methods

2.1. Materials

Cbz-Phe(4F) was purchased from GL Biochem (Shanghai) Ltd. with a purity > 95 %. Cbz-Phe, Fmoc-Phe, and Fmoc-Phe(4F) were purchased from Bachem AG (Bubendorf, Switzerland) Co., Ltd. with a purity of 98 %. Methanol and sodium dodecyl sulfate (SDS) were purchased from Sigma-Aldrich (St. Louis, Missouri, USA). All reagents were analytical purity grade.

2.2. Self-assembly of Cbz-Phe(4F)

Cbz-Phe(4F) was first dissolved in pure methanol at a concentration of 50 mg/mL and then diluted with distilled water to allow the self-assembly. The final concentration was 2 mg/mL.

2.3. Optical microscopy

Cbz-Phe(4F) solution was added on a glass slide for observation. The images were recorded by an optical microscope (Axio Scope.A1, Carl Zeiss, Germany).

2.4. Scanning electron microscopy (SEM)

First, 20 μ L of Cbz-Phe(4F) solution (2 mg/mL) was drop-casted on a clean silicon substrate and then dried in the hood. Then, the sample was coated using a Polaron SC7640 sputter coater (10 mA, 60 s). Scanning electron microscopy (SEM) images were recorded using an analytical high-resolution scanning electron microscope Apreo 2S (Thermo Fisher Scientific). The accelerating voltage was 2 kV.

2.5. Fourier transform infrared spectroscopy (FT-IR)

FT-IR was recorded using a Nicolet 6700 FT-IR spectrometer with a deuterated triglycine sulfate (DTGS) detector (Thermo Fisher Scientific, MA, USA) at a 4 cm $^{-1}$ resolution and averaged after 2000 scans. The sample was deposited on a CaF $_2$ plate and dried by vacuum. Then, the peptide deposits were resuspended with D $_2$ O and subsequently dried. The resuspension procedure was repeated twice to ensure maximal hydrogen-to-deuterium exchange.

2.6. Circular dichroism (CD)

The CD spectra were collected in a J-810 spectropolarimeter (JASCO, Tokyo, Japan), using a 0.1 cm pathlength quartz cuvette for far-UV CD spectroscopy (in the spectral range between 190 and 260 nm with a step width of 0.05 nm) at 25 $^{\circ}\text{C}$. The concentration of Cbz-Phe(4F) was 0.1 mg/mL.

2.7. All-atomic molecular dynamics (MD) simulations for the self-assembly of Cbz-Phe(4F)

A Cbz-Phe(4F) molecule model was created with GaussView 6; then the geometrical optimization and frequency calculation were performed with the Gaussian 16 package, [25] where the M06-2X functional and 6-311G** basis sets were applied [26,27]. DFT-D3 was involved in dispersion corrections. Topology of the Cbz-Phe(4F) molecule was created through the Soptop package (Tian Lu, Sobtop, Version 1.0 (dev3.1), https://sobereva.com/soft/Sobtop (accessed on 26/03/2023)) from the results of the optimization and frequency analyses. The atomic coordinates were used to create the topology of the molecule with Generation Amber Force Field (GAFF) and the bonded parameters were calculated from the Hessian matrix obtained from frequency analyses [28]. The single point energy calculation was performed using Gaussian 16 at the level of B2PLYP/6-311G** with DFT-D3 BJ Damp as dispersion corrections. Using the results of the single point energy, wave function analyses were performed using the Multiwfn package [29]; the Restrained ElectroStatic Potential (RESP) charges [30] were obtained and used for further MD simulations for the Cbz-Phe(4F) molecule. All calculations were applied with the SMD implicit solvent model with water as the solvent. The GROMACS MD package (version 5.1.4) was used for the MD simulations of Cbz-Phe(4F) [31]. Cubic periodic boxes of size 10*10*10 nm³ were created to accommodate 400 Cbz-Phe(4F) molecules; then the box was filled with TIP3P water molecules. The system energy was minimized by the steepest descent algorithm. Then, the system was equilibrated in NVT and NPT ensembles (T = 300 K, P =1.0 bar) for 0.2 ns with a Berendsen thermostat and a Berendsen barostat [32]. The calculations of the long-distance electrostatic interactions and the constraints of all the covalent bond lengths were based on the particle mesh Ewald (PME) method and the LINCS algorithm, respectively [33]. Moreover, the cutoff distances of short-range electrostatic and van der Waals interactions were set as 1.0 nm. The simulation was performed for 200 ns (the total energy was constant during the first 100 ns, suggesting that the states of the system were stable (Figure S3b). The radial distribution functions (RDFs) and the hydrogen bonds were calculated by averaging the frames from the last 10 ns of the 200 ns trajectories.

2.8. Self-assembly of Cbz-Phe(4F) on different substrates

The polydimethylsiloxane (PDMS), silicon, glass, titanium (50 nm), gold (50 nm), and polyethylene substrates with a size of $1\!\!^*1$ cm 2 were sonicated for 15 min with ethanol and then washed with distilled water. Then, the surfaces were dried by a flow of N_2 . Next, 100 μL of Cbz-Phe (4F) with a concentration of 2 mg/mL was drop-casted on each substrate. The water contact angle and rolling angle were measured using a Theta Lite optical tensiometer (Attension, Finland). The water used for this measurement was Milli-Q water from a Millipore System (Marlborough, France). The droplet volume was 8 μL . All the measurements are based on 9 repeats.

2.9. Preparation of self-standing Cbz-Phe(4F) materials

A cleaned PDMS substrate (1*1 cm 2) was prepared as described above. A 100 μ L drop of self-assembled Cbz-Phe(4F) solution (2 mg/mL) was drop-casted on a PDMS substrate and then dried at room temperature. The self-standing Cbz-Phe(4F) material was prepared by drop-

casting three times as described and then was taken from the PDMS substrate by tweezers. The optical microscope image, SEM image and the water contact angle were recorded.

2.10. Mechanical properties of self-standing Cbz-Phe(4F)

(1) Rheological test: The storage modulus (G') and the loss modulus (G'') were determined using a parallel-plate HAAKE RheoScope-1 rheometer (Thermo Haake, Langenselbold, Germany). According to our preliminary experiments (Figure S4a), a strain of 0.5 % laid in the linear viscoelastic region of Cbz-Phe(4F). Therefore, time sweep oscillation tests were performed at a constant strain (0.5 %) and a constant sweep (1 Hz) at room temperature. The gap distance and the diameter of the petri dishes were 1 mm and 25 mm, respectively. (2) Atomic force microscope (AFM) measurement: Young's modulus and point stiffness were recorded by fitting the approaching curve to the Hertz model. Briefly, AFM experiments were carried out by a Dimension Icon XR Scanning Probe Microscope (Bruker). An indentation experiment was performed, with the microscope employed in force curve mode, and the deflection (force) of the cantilever was plotted as a function of the sample height. The stiffness and Young's modulus were acquired in PF-ONM (Peak-Force Quantitative Nanoscale Mechanical characterization) by using a PDNISP diamond probe (k = 150 N/m, Bruker). The cantilever was moved over the self-standing Cbz-Phe(4F) at a speed of 2 µm s⁻¹ and then was retracted to move to another area. (3) Tensile strength measurement: The tensile strength of self-standing Cbz-Phe(4F) was determined by conducting a standard uniaxial tensile experiment. The sample was fixed on the tensile instrument and the dynamic force during the stretching process was recorded. The distances between the two grips and the loading speed were 5 mm and 0.1 mm/s, respectively. (4) Finger-wipe stability: the self-standing Cbz-Phe(4F) material was wiped with a finger at a load of 1 g. The water contact angle and rolling angle were measured.

2.11. Stability of self-standing Cbz-Phe(4F) materials

The thermal, chemical, and proteolytic resistance of the self-standing Cbz-Phe(4F) was determined. All samples after above treatments were investigated by SEM, HPLC (High-performance liquid chromatography), mass spectroscopy (MS) and water contact angle measurements. (1) Thermal stability: The self-standing Cbz-Phe(4F) material was investigated by treating it at 100 °C for 12 h. To better understand the thermal behavior, differential scanning calorimetry (DSC) and thermogravimetric analysis (TGA) of self-standing Cbz-Phe(4F) were carried out using DSC (NETZSCH) and thermogravimetric analyzer Q50 (TA Instrument, DE). The material was performed under a temperature range of 30-500 °C and at a scanning rate of 20 °C min⁻¹ under a nitrogen environment. (2) Chemical stability: To study the chemical stability, the self-standing Cbz-Phe(4F) was immersed in hydrochloric acid (pH = 1), sodium hydroxide (pH = 14), and 1 % sodium dodecyl sulfate (SDS) solution for 12 h and then dried under ambient conditions. (3) Stability to enzymatic proteolysis: Proteinase-K solution was prepared by dissolving the enzyme at 20 U mL^{-1} in 50 mM tris buffer (pH 8.0, 5 mM CaCl2). The HPLC analysis was performed using Waters e2695 with a C18 LC column (5 μ m, 110 Å, 250 \times 4.6 mm). The parameters were as follows: the mobile phase consisted of acetonitrile/water (60:40, v/v); the wavelength was 229 nm, and the flow rate was set at 1.0 mL min^{-1} . The mass analysis was characterized by electron spray ionization mass spectroscopy using an LCQ Fleet Ion Trap mass spectrometer (Thermo Fisher Scientific, Waltham, MA USA).

3. Results and discussion

It was demonstrated that changing the position of just one fluorine atom in a sequence can dramatically alter the hydrophobicity, amphiphilicity, and secondary structure of peptide chains [34]. Moreover, leveraging the fluorous effect to direct the peptide assembly resulted in an entirely new class of building blocks from which unique and bioactive materials can be constructed [34]. Herein, we designed a functionalized amino acid (Cbz-Phe(4F)) containing a fluorinated phenylalanine and a functionalized benzyloxycarbonyl (Cbz) group (Fig. 1). Cbz, as the simplest functionalized aromatic group, can provide not only the driving force for the self-assembly but also the hydrophobicity. Modifying the phenylalanine residue with fluorine also increases the hydrophobicity of the amino acid. Our previous study demonstrated that di-/tripeptides containing Phe(4F) residue exhibit low cytotoxicity and high biocompatibility [35,36]. To self-assemble the functionalized amino acid, we dissolved Cbz-Phe(4F) in methanol and then diluted it using distilled water to a concentration of 2 mg/mL. Similar self-assembled fibrillar structures could also be detected using a lower concentration (0.5 mg/ mL) (Figure S1). The self-assembly of Cbz-Phe(4F) was studied experimentally and by all-atomic molecular dynamics (MD) simulations. Then, the self-assembled structures were drop-casted on different substrates and the surface was endowed with superhydrophobicity. When the selfassemblies were deposited on the substrates 3 times, a self-standing superhydrophobic material was obtained (Fig. 1).

3.1. Self-assembly of Cbz-Phe(4F) in solution and on substrates

To study the self-assembly of Cbz-Phe(4F), optical microscope and SEM analysiswere performed. As shown in Fig. 2a-b, Cbz-Phe(4F) selfassembled into fibers with a diameter of 1 \sim 5 μm . The self-assembly process could be driven by side-chain π - π stacking of the Cbz group and Phe(4F) residue as well as hydrogen bonding between the amide groups (detailed information is in the MD simulation section). For dynamic monitoring of the self-assembly process, optical microscope images were recorded immediately after diluting the amino acid. From Figure S2, it can be observed that fibers gradually lengthen and then form a crosslinked network with time. Fibrils could be detected within 30 s after dilution, indicating fast self-assembly kinetics. This rate was previously reported for other peptides and/or functionalized amino acids with hydrophobicity and aromaticity [19]. To gain information on the conformation of the assemblies, circular dichroism (CD) and fourier transform infrared spectroscopy (FTIR) were carried out. The CD spectra had a positive peak at around 195 nm and another strong positive band at 217 nm, suggesting a β-turn conformation (Fig. 2c). Similar CD spectral features were observed for other aromatic peptides that assumed a β-turn conformation (e.g., Phe-ΔPhe, Ala-Pro-Tyr-Gly-NHCH₃, and Leu-Pro-Tyr-Ala-NHCH₃) [37,38]. FT-IR analysis was performed to further ascertain the results obtained from the CD spectra. As shown in Fig. 2d, it was noted that there was a strong shoulder at around 1690 cm^{-1} in the amide I band ($1600-1800 \text{ cm}^{-1}$, the C=O stretching vibration), suggesting a β-turn conformation for the assemblies. Chauhan et al. reported that Phe-ΔPhe nanotubes exhibit a strong peak at around 1690 cm⁻¹, which was identified as a β -turn structure [37]. In addition, two other weak absorption peaks at 1636 cm⁻¹ and 1653 cm⁻¹

are also related to a β -turn conformation [39,40]. These findings are consistent with the observation from the CD spectrum.

The self-assembly of amino acids and peptides on a solid support is an important way to fabricate functional materials [41,42]. The selfassembled Cbz-Phe(4F) was drop-casted on different substrates including PDMS, silicon, glass, Ti (50 nm), Au (50 nm), and polyethylene substrates with a size of 1 cm² and then dried at room temperature. As shown in Fig. 2e-f, the water contact angle of the PDMS, silicon, glass, Ti, Au, and polyethylene substrates modified with the assemblies was 155 \pm 4°, 149 \pm 3°, 144 \pm 5°, 146 \pm 2°, 148 \pm 4°, and $147\pm3^{\circ},$ respectively. The differences in the values of the water contact angle on the different substrates result from the substrate properties. It has been reported that the hydrophobicity of a certain substrate can affect the peptide/amino acid assemblies [43]. On the hydrophobic PDMS substrate, the arrangement of Cbz-Phe(4F) assemblies resulted in a water contact angle larger than 150°. We also measured the rolling angle of the different substrates modified by the assemblies. As shown in Table S1, only a modified PDMS surface showed a rolling angle lower than 10°. This indicated that the assemblies formed by Cbz-Phe(4F) endowed the PDMS substrate with superhydrophobicity. It has been reported that superhydrophobic coating can be achieved using two parameters, low surface energy provided by chemical moieties and hierarchical structure [2,44]. The Cbz-Phe(4F) molecule with its two aromatic moieties, one of them modified by a fluorine atom provides a low surface energy chemistry. Besides, the self-assemblies on the surface with a random arrangement of fibrous structures (Fig. 2b) provide the surface roughness. We also compared the water contact angle of PDMS surfaces drop-casted with Cbz-Phe, Fmoc-Phe, or Fmoc-Phe(4F) with that of Cbz-Phe(4F). The results are shown in Table S2. The PDMS cast with Cbz-Phe had a water contact angle of $108 \pm 3^{\circ}$, which is lower than the one obtained for the fluorinated amino acid. This suggests that introducing fluorine into Cbz-Phe(4F) molecules enhances the hydrophobicity of the assemblies. It was reported that the presence of fluorine atoms within peptides can often favorably alter the biophysical and chemical properties, such as hydrophobicity, acidity/basicity, reactivity, and conformation [34,45]. Moreover, Fmoc-Phe and Fmoc-Phe (4F) showed a water contact angle of 110 \pm 2° and 128 \pm 4°, indicating that Cbz-functionalized amino acid was inclined to self-assemble into superhydrophobic structures. These findings indicate the superhydrophobic properties of Cbz-Phe(4F), displaying sufficient superhydrophobicity on solid surfaces, which can be useful for further generating superhydrophobic coatings/surfaces when compared to other functionalized phenylalanine amino acids.

3.2. Molecular simulation for Cbz-Phe(4F) self-assembly

To illustrate the structures and interactions of the assemblies formed by Cbz-Phe(4F), all-atomic molecular dynamics (MD) simulations were performed. The architectures of Cbz-Phe(4F) are shown in Fig. 3a. It was found that Cbz-Phe(4F) aggregates and forms long fibril assemblies,

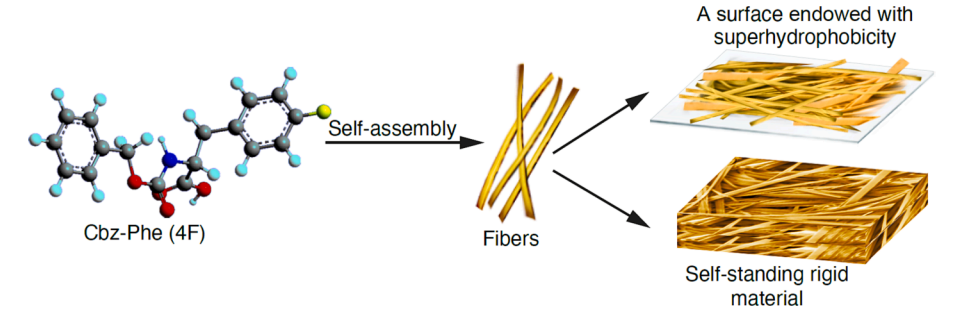


Fig. 1. The scheme illustrates the self-assembly of Cbz-Phe(4F) and the formation of self-standing superhydrophobic material made of Cbz-Phe(4F). Cbz-Phe(4F) can self-assemble into fibrous structures on the solid substrates and endow the substrates with superhydrophobicity. To generate superhydrophobic materials, the self-standing superhydrophobic material was formed by drop-casting Cbz-Phe(4F) on a PDMS substrate three times.

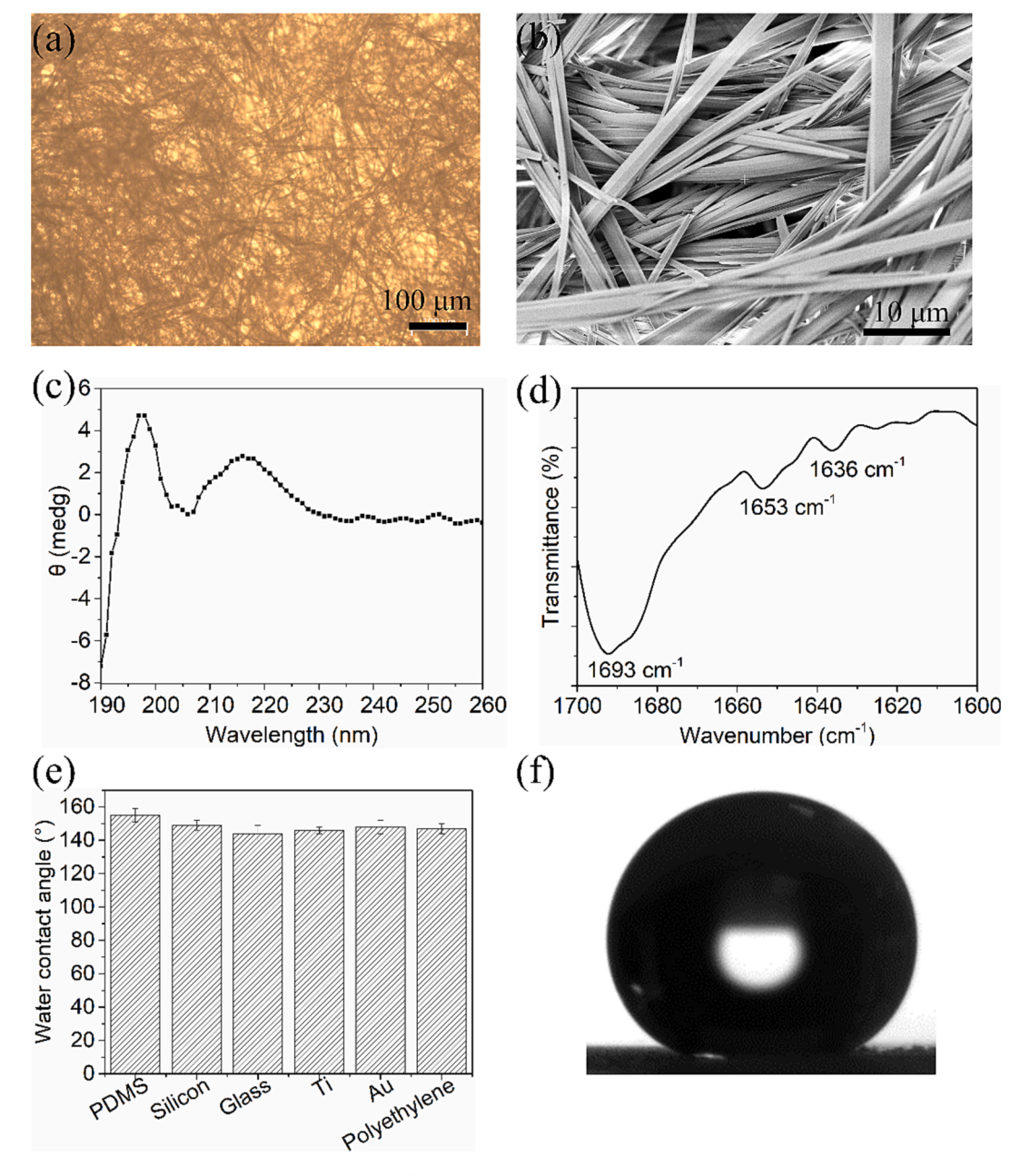


Fig. 2. (a) Optical microscope images and (b) SEM images of the self-assembled structures formed by Cbz-Phe(4F), (c) Circular dichroism (CD) spectrum (190–260 nm) of the assemblies formed by Cbz-Phe(4F), where the peak position can provide the structural information of assemblies, (d) Fourier Transform Infrared Spectroscopy (FT-IR) spectrum (1600–1700 cm⁻¹) of the assemblies formed by Cbz-Phe(4F), where the peak around 1600–1700 cm⁻¹ also provides the structural information for these assemblies, (e) the water contact angle for different substrates (PDMS, Silicon, Glass, Ti, Au, and Polyethylene substrates) modified with Cbz-Phe(4F), and (f) the representative image of the water contact angle measurement on the PDMS substrate (water contact angle > 150°). SD was based on 9 repeats.

accounting for the fibrous structures observed using an optical microscope and SEM (Fig. 2a-b). The RDF/g(r) for the Cbz-Phe(4F) molecules in the system is shown in Fig. 3b. The g(r) value is larger than 1, indicating aggregations of the Cbz-Phe(4F) molecules. Two peaks are located at around 0.5 nm and 1 nm in the g(r) profile, respectively, indicating two different packing patterns of Cbz-Phe(4F). The simulations (Fig. S3a) revealed that there were $80 \sim 100$ hydrogen bonds between 400 Cbz-Phe(4F) molecules. According to the results of g(r) and based on the number of hydrogen bonds, we suggest that the backbone of Cbz-Phe(4F) aggregations (Fig. 3c) is stabilized through hydrogen bonds, whereas the isotropic growth (Fig. 3d) of the aggregates is driven by hydrophobic interactions. Such a proposal can be confirmed by the observations from the architecture of the Cbz-Phe(4F) aggregations. As shown in Fig. 3c-d, the center of mass of each Cbz-Phe(4F) molecule was

denoted by orange spheres, which were connected if their distances were smaller than 0.5 nm (Fig. 3c) or 1.0 nm (Fig. 3d). Fig. 3c shows that the centroids within a distance of 0.5 nm were linked in a "single-single" pattern, corresponding to the formation of the backbone of the aggregates. On the other hand, numerous centroids within a distance of 1 nm were connected with a "single-multiple" pattern, leading to the isotropic growth of the aggregates. Such observations might illustrate the results of g(r) and the number of hydrogen bond analyses. We also noted that the potential and the total energy of the simulation system were constant during simulation, and we think that the system was in a (meta-)stable state (Figure S3b). Since the gyration radius (Rg) of a polymer revealed the molecular size in different dimensions, Rg values were determined during the aggregation of those Cbz-Phe(4F) molecules as shown in Figure S3c. Given that Cbz-Phe(4F) molecules were distributed evenly

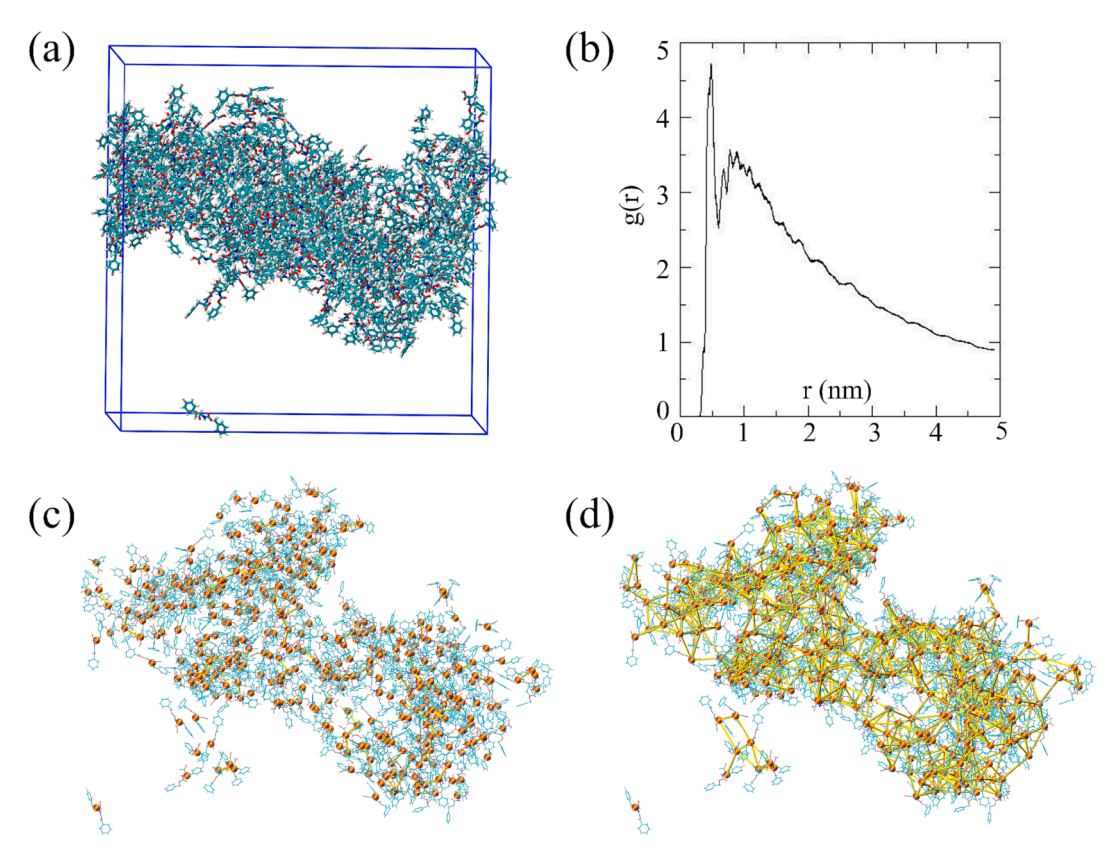


Fig. 3. The all-atomic molecular dynamics simulations of self-assembled Cbz-Phe(4F). The Cbz-Phe (4F) architecture of (a) Representative aggregations, (b) RDF/g (r) of Cbz-Phe (4F) molecular, (c) molecular centroids within 0.5 nm connected by a yellow rod, and (d) molecular centroids within 1 nm connected by a yellow rod.

and randomly in the simulation box, the initial values of Rg in X-, Y- and Z-directions should be close to each other, as observed from the beginning of the simulations. After around 500 ps of simulations, however,

 Rg_X and Rg_Z decreased, while there was little change in Rg_Y during the whole simulations. Such observations indicated that those Cbz-Phe(4F) molecules aggregated from X- and Z-directions and the aggregates

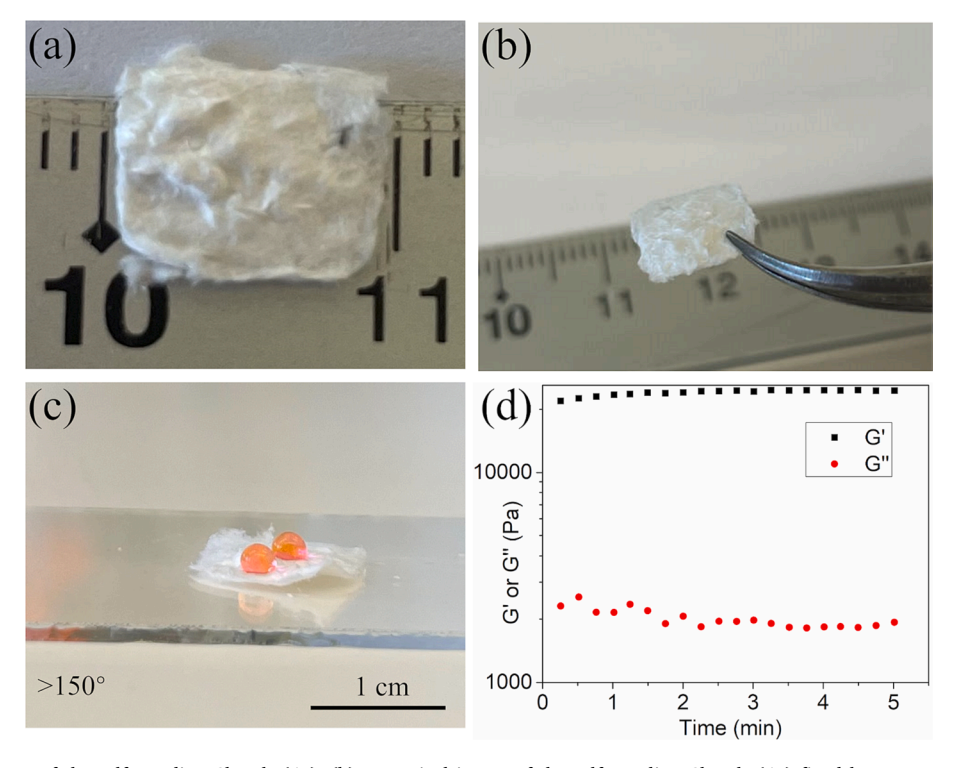


Fig. 4. (a) An optical image of the self-standing Cbz-Phe(4F), (b) an optical image of the self-standing Cbz-Phe(4F) fixed by tweezers, (c) photograph of water droplets dyed by Rhodamine B on self-standing Cbz-Phe(4F), and (d) storage modulus of self-standing Cbz-Phe(4F) material.

expanded in Y-direction. The snapshot of MD simulations exhibited the self-assembly of Cbz-Phe(4F) more straightforwardly. It was supposed that Cbz-Phe(4F) molecules first formed the structural backbone by hydrogen bonds and then the aggregates expanded non-isotropically. String-like aggregates were formed mainly by hydrophobic interactions, which would further lead to the long fibrous structures at the macro scale.

3.3. Characterization and mechanical properties of self-standing Cbz-Phe (4F) materials

To generate a self-standing superhydrophobic material, we dropcasted the assemblies formed by Cbz-Phe(4F) on a PDMS substrate (1 cm²) 3 times. Then, the dried assemblies could be easily removed from the substrate using tweezers. This process resulted in a white self-standing material (Fig. 4a-b). Moreover, this self-standing Cbz-Phe (4F) material had a water contact angle larger than $152^{\circ}\pm2^{\circ}$ (Fig. 4c). The optical microscope image and SEM image revealed the formation of a microfiber network with a diameter of $1-5~\mu m$ formed by Cbz-Phe(4F) (Figure S4b and Fig. 5a). To investigate its mechanical properties, the rheology, AFM, and tensile strength were determined. Fig. 4d shows that the G' value was significantly higher than the G' value, suggesting the elastic solid behavior of self-standing Cbz-Phe(4F) [46]. The average G' and G' values were 2.4 ± 0.8 kPa and 0.2 ± 0.02 kPa, respectively; the G' value was significantly higher than the G' value. These results indicate that the self-standing Cbz-Phe(4F) has high rigidity; the G' value of Cbz-Phe(4F) was comparable to that of peptide amphiphile hydrogels and functionalized amino acid/dipeptide hydrogels [47,48].

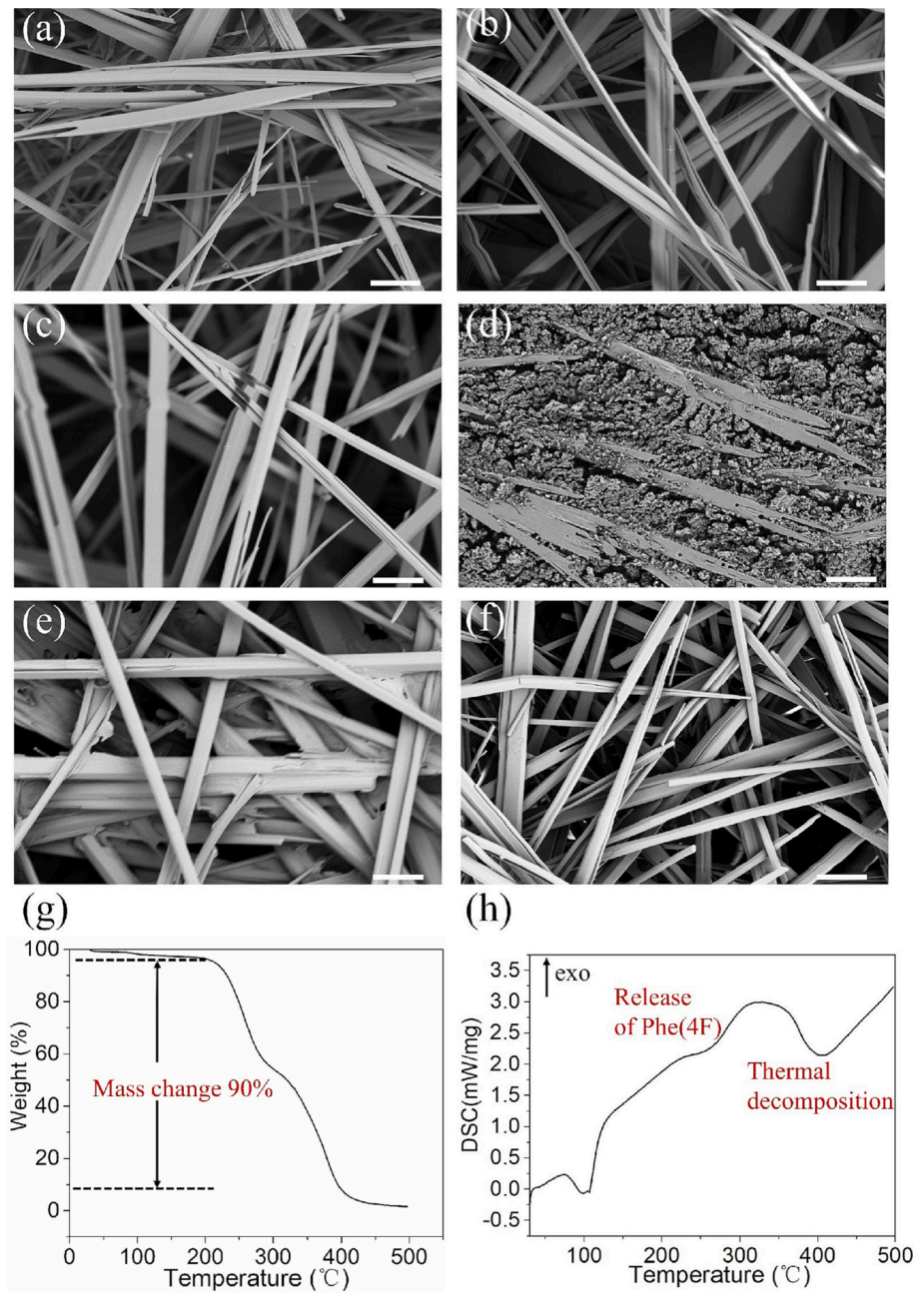


Fig. 5. SEM images of the self-standing Cbz-Phe(4F) (a) Untreated, (b) Treated with 1 % sodium dodecyl sulfate (SDS) for 12 h, (c) Treated with hydrochloric acid (pH = 1) for 12 h, (d) Treated with sodium hydroxide (pH = 14) for 12 h, (e) Digested by proteinase K (20 U mL $^{-1}$), and (f) Treated by heating at 100 °C for 12 h. Thermal analysis of self-standing Cbz-Phe(4F) was characterized by (g) TGA and (h) DSC. The scale bar represents 10 μ m.

Next, we also characterized the mechanical properties using AFM (Figure S4c). Typically, the cantilever approached the self-standing Cbz-Phe(4F) and retracted at a constant speed; Young's modulus was obtained by fitting the force-distance traces with the Hertz model [16]. The measured elasticity of self-standing Cbz-Phe(4F) had a Young's modulus of 53 \pm 10 GPa and a stiffness of 449 \pm 58 N/m, indicating rigid mechanics. The observed value of Young's modulus was significantly higher than that of some other biomaterials reported previously, such as L-Phe fibers (5.8 GPa), DNA-based structures (0.3-2 GPa), and insulin self-assembling nanofibers (0.28 GPa) [16,49,50]. The stiffness value of Cbz-Phe(4F) self-standing material was also greater than that of diphenylalanine nanotubes (150 N/m) and Boc-Phe-Phe-OH spheres (430 N/ $\,$ m) [51,52]. We suggest that the stiffness stems from the strong molecular packing and aggregations (Fig. 3). Moreover, the tensile strength of self-standing Cbz-Phe(4F) was also evaluated. As shown in Figure S4d, the force was rapidly increased in the first 0.2 mm and then decreased, indicating that the structure initially was destroyed at a displacement of 0.2 mm. The peak force was 0.015 N, suggesting the weak tensile strength of self-standing Cbz-Phe(4F). We propose that the structure of the materials consisted of self-assembling fibrous aggregation and stacking, where the assemblies were stabilized by non-covalent interactions. Our self-standing functionalized Cbz-Phe(4F) with superhydrophobic properties can serve as a novel superhydrophobic material.

3.4. Chemical and thermal stability of self-standing Cbz-Phe(4F) materials

We investigated the chemical, thermal, and enzymatic stability of self-standing Cbz-Phe(4F). For chemical stability, self-standing Cbz-Phe (4F) was incubated in hydrochloric acid (pH = 1), sodium hydroxide (pH = 14), and 1 % sodium dodecyl sulfate (SDS) solution for 12 h. As shown in Fig. 5a, the untreated self-standing Cbz-Phe(4F) showed a microfibrous network with a diameter of 1-5 μm. Fig. 5b-c shows that self-standing Cbz-Phe(4F) maintained its structural integrity after treatment by 1 % SDS and HCl (pH = 1), indicating a high stability under these conditions. Moreover, it can be also seen from Table S3 that the peak position of HPLC and the mass-to-charge ratio (m/z) did not change, compared to the untreated sample. It was observed that the Cbz-Phe(4F) microfibers had almost disintegrated after treatment with a basic solution (Fig. 5d). However, the HPLC and MS results were similar to those of the untreated sample. These results indicate that Cbz-Phe(4F) had disassembled under a basic environment rather than changing its molecular composition. When applying peptide-/amino acid-based functional materials, enzymatical stability is desirable [53]. Fig. 5e shows that no notable variations could be observed before and after incubating the self-standing Cbz-Phe(4F) with the enzyme, suggesting that the Cbz-Phe(4F) material showed resistance to enzymatic proteolysis. Furthermore, thermal stability is another key factor in evaluating the stabilities of functional materials. As shown in Fig. 5f and Table S3, the structure, peak position of HPLC, and the m/z did not change when exposed to 100 °C for 12 h. To investigate the superhydrophobicity after chemical and thermal treatment, we measured the water contact angle and rolling angle after chemical and thermal treatments. It was clear that the self-standing Cbz-Phe(4F) material was stable and remained superhydrophobic after chemical and thermal treatments besides the treatment with NaOH. To further study the thermal stability, the selfstanding of Cbz-Phe(4F) was investigated using DSC and TGA. As shown in Fig. 5g-h, the DSC and TGA thermogram showed that the Cbz-Phe(4F) residue had completely decomposed at around 400 °C. Moreover, it was also observed that the self-standing Cbz-Phe(4F) maintained stability under 200 °C (Fig. 5g), which confirmed the results of thermal stability at 100 °C (Fig. 5f and Table S3). Importantly, self-standing Cbz-Phe(4F) presented an endothermic DSC peak at 300 °C, which could correspond to the release of Phe(4F) residue. Other studies revealed that the release of phenylalanine (Phe) residue in diphenylalanine was presented at 175 °C [42]. This suggests that introducing fluorine into phenylalanine residue could enhance the stability of amino acids and/or peptides. It was also noted that an endothermic peak was centered at 100 °C, which could be attributed to the evaporation of residual distilled water from the self-standing Cbz-Phe(4F). Subsequently, we also performed a finger-wipe test for the self-standing Cbz-Phe(4F). As shown in Table S4, the water contact angle and rolling angle did not decrease after finger-wipe with a load force of 1 g. This indicated that the coating has good mechanical stability. These results indicated that the self-standing Cbz-Phe(4F) exhibited high stability and sufficiently high rigidity, which can be utilized in biomaterial applications.

4. Conclusions

In this work, we designed a functionalized amino acid that can selfassemble into a self-standing superhydrophobic material. This amino acid, Cbz-Phe(4F), self-assembled into microfibers with β-turn structures in the aqueous phase. According to MD simulations, the formation of the fibers is governed by hydrogen bonds along with hydrophobic interactions (mainly $\pi - \pi$ stacking). Cbz-Phe(4F) molecules first aggregate to form a fibrous backbone by hydrogen bonds and then became isotropic by hydrophobic interactions. Moreover, Cbz-Phe(4F) can endow different substrates with superhydrophobic properties (water contact angle $>150^{\circ}\mbox{)}.$ Interestingly, when we drop-casted the Cbz-Phe (4F) assemblies three times on the substrates, self-standing rigid materials with superhydrophobicity were formed. The self-standing Cbz-Phe (4F) had high rigidity, with a Young's modulus of 52.86 GPa. Importantly, the self-standing Cbz-Phe(4F) was stable against proteinase K digestion, thermal treatment, harsh acid environment, and the surfactant SDS

We describe, for the first time, the self-assembly of an individual amino acid into a self-standing superhydrophobic material. Compared to other synthesized materials, [4,6,7,54] the self-assembly of amino acids into superhydrophobic materials broadens the scope of application of superhydrophobic materials due to their inherent biocompatibility and biodegradation. Moreover, the low manufacturing cost and simple process method (by drop-casting) of Cbz-Phe(4F) provide an adequate large-scale production track for superhydrophobic materials. Importantly, this self-standing superhydrophobic material has a remarkable mechanical strength, which is more than ten times higher than other biomolecular self-assemblies [16,49,50]. Moreover, this superhydrophobic material has high chemical, enzymatic and thermal stability, therefore it is more durable than thin superhydrophobic coatings. As a self-standing three-dimensional (3D) superhydrophobic material, this compound can be useful for drug delivery, as a barrier in different devices and as an adsorber of hydrophobic contaminants [55,56]. Our work provides a novel strategy for the design and development of attractive and smart superhydrophobic materials using simple selfassembling amino acids.

CRediT authorship contribution statement

Tan Hu: Conceptualization, Methodology, Investigation, Writing – original draft. **Zhuo Zhang:** Resources, Software. **Meital Reches:** Conceptualization, Methodology, Writing – review & editing, Supervision, Funding acquisition.

Declaration of Competing Interest

The authors declare that they have no known competing financial interests or personal relationships that could have appeared to influence the work reported in this paper.

Data availability

Data will be made available on request.

Acknowledgments

This research was supported by grants from the National Research Foundation, Prime Minister's Office, Singapore under its Campus of Research Excellence and Technological Enterprise (CREATE) programme. ZZ acknowledges the research funds from the National Natural Science Foundation of China (32172350). We also would like to thank Dr. Anna Radko for her assistance with the AFM measurements.

Appendix A. Supplementary data

Supplementary data to this article can be found online at https://doi.org/10.1016/j.jcis.2023.11.062.

References

- M. Ruzi, N. Celik, M.S. Onses, Superhydrophobic coatings for food packaging applications: A review, Food Packag. Shelf Life. 32 (2022) 100823.
- [2] L. Wang, X. Guo, H. Zhang, Y. Liu, Y. Wang, K. Liu, H. Liang, W. Ming, Recent advances in superhydrophobic and antibacterial coatings for biomedical materials, Coatings. 12 (2022) 1469.
- [3] Y. Bai, H. Zhang, Y. Shao, H. Zhang, J. Zhu, Recent progresses of superhydrophobic coatings in different application fields: An overview, Coatings. 11 (2021) 116, https://doi.org/10.3390/coatings11020116.
- [4] A. Milionis, E. Loth, I.S. Bayer, Recent advances in the mechanical durability of superhydrophobic materials, Adv. Colloid Interface Sci. 229 (2016) 57–79, https:// doi.org/10.1016/j.cis.2015.12.007.
- [5] I.S. Bayer, Superhydrophobic coatings from ecofriendly materials and processes: A review, Adv. Mater. Interfaces. 7 (2020) 2000095, https://doi.org/10.1002/ admij.20200095
- [6] A. Hooda, M.S. Goyat, J.K. Pandey, A. Kumar, R. Gupta, A review on fundamentals, constraints and fabrication techniques of superhydrophobic coatings, Prog. Org. Coatings. 142 (2020) 105557, https://doi.org/10.1016/j.porgcoat.2020.105557.
- [7] Q. Zeng, H. Zhou, J. Huang, Z. Guo, Review on the recent development of durable superhydrophobic materials for practical applications, Nanoscale 13 (2021) 11734–11764, https://doi.org/10.1039/D1NR01936H.
- [8] A.R. Bagheri, C. Laforsch, A. Greiner, S. Agarwal, Fate of So-called biodegradable polymers in seawater and freshwater, Glob. Challenges. 1 (2017) 1700048, https:// doi.org/10.1002/gch2.201700048.
- [9] I. Tagliaro, S. Seccia, B. Pellegrini, S. Bertini, C. Antonini, Chitosan-based coatings with tunable transparency and superhydrophobicity: A solvent-free and fluorinefree approach by stearoyl derivatization, Carbohydr. Polym. 302 (2023) 120424, https://doi.org/10.1016/j.carbpol.2022.120424.
- [10] Y. Wang, Z. Li, J. Wang, J. Wang, X. Li, C. Kuang, Superhydrophobic coating constructed from rosin acid and TiO2 used as blood repellent dressing, Mater. Des. 222 (2022) 111072, https://doi.org/10.1016/j.matdes.2022.111072.
- [11] J.S. Lee, J. Ryu, C.B. Park, Bio-inspired fabrication of superhydrophobic surfaces through peptide self-assembly, Soft Matter 5 (2009) 2717–2720, https://doi.org/ 10.1020/89087823
- [12] Y. Chen, K. Tao, W. Ji, V.B. Kumar, S. Rencus-Lazar, E. Gazit, Histidine as a key modulator of molecular self-assembly: Peptide-based supramolecular materials inspired by biological systems, Mater. Today. 60 (2022) 106–127, https://doi.org/ 10.1016/j.mattod.2022.08.011.
- [13] Y. Wang, Q. Geng, Y. Zhang, L. Adler-Abramovich, X. Fan, D. Mei, E. Gazit, K. Tao, Fmoc-diphenylalanine gelating nanoarchitectonics: A simplistic peptide selfassembly to meet complex applications, J. Colloid Interface Sci. 636 (2023) 113–133, https://doi.org/10.1016/j.jcis.2022.12.166.
- [14] Y. Huo, J. Hu, Y. Yin, P. Liu, K. Cai, W. Ji, Self-assembling peptide-based functional biomaterials, Chembiochem. 24 (2023), https://doi.org/10.1002/cbic.202200582 e202200582.
- [15] P. Chakraborty, E. Gazit, Amino acid based self-assembled nanostructures: Complex structures from remarkably simple building blocks, ChemNanoMat. 4 (2018) 730–740, https://doi.org/10.1002/cnma.201800147.
- [16] S. Bera, B. Xue, P. Rehak, G. Jacoby, W. Ji, L.J.W. Shimon, R. Beck, P. Král, Y. Cao, E. Gazit, Self-assembly of aromatic amino acid enantiomers into supramolecular materials of high rigidity, ACS Nano. 14 (2020) 1694–1706, https://doi.org/ 10.1021/acsnano.9b07307.
- [17] P. Singh, S.K. Brar, M. Bajaj, N. Narang, V.S. Mithu, O.P. Katare, N. Wangoo, R. K. Sharma, Self-assembly of aromatic α-amino acids into amyloid inspired nano/micro scaled architects, Mater. Sci. Eng. c. 72 (2017) 590–600, https://doi.org/10.1016/j.msec.2016.11.117.
- [18] D. Banik, A. Roy, N. Kundu, N. Sarkar, Modulation of the excited-state dynamics of 2,2'-Bipyridine-3,3'-diol in Crown Ethers: A possible way to control the morphology of a glycine fibril through fluorescence lifetime imaging microscopy, J. Phys. Chem. b. 120 (2016) 11247–11255, https://doi.org/10.1021/acs.jpcb.6b07524.
- [19] K. Tao, A. Levin, L. Adler-Abramovich, E. Gazit, Fmoc-modified amino acids and short peptides: Simple bio-inspired building blocks for the fabrication of functional materials, Chem. Soc. Rev. 45 (2016) 3935–3953.
- [20] S.-M. Hsu, F.-Y. Wu, H. Cheng, Y.-T. Huang, Y.-R. Hsieh, D.-T.-H. Tseng, M.-Y. Yeh, S.-C. Hung, H.-C. Lin, Functional supramolecular polymers: A fluorescent microfibrous network in a supramolecular hydrogel for high-contrast live cell-

- material imaging in 3D environments, Adv. Healthc. Mater. 5 (2016) 2406–2412, https://doi.org/10.1002/adhm.201600342.
- [21] T. Imae, Y. Takahashi, H. Muramatsu, Formation of fibrous molecular assemblies by amino acid surfactants in water, J. Am. Chem. Soc. 114 (1992) 3414–3419.
- [22] F. Clerici, E. Erba, M.L. Gelmi, S. Pellegrino, Non-standard amino acids and peptides: From self-assembly to nanomaterials, Tetrahedron Lett. 57 (2016) 5540–5550, https://doi.org/10.1016/j.tetlet.2016.11.022.
- [23] S. Guerin, A. Stapleton, D. Chovan, R. Mouras, M. Gleeson, C. McKeown, M. R. Noor, C. Silien, F.M.F. Rhen, A.L. Kholkin, N. Liu, T. Soulimane, S.A.M. Tofail, D. Thompson, Control of piezoelectricity in amino acids by supramolecular packing, Nat. Mater. 17 (2018) 180–186, https://doi.org/10.1038/nmat5045.
- [24] A. Pizzi, L. Lascialfari, N. Demitri, A. Bertolani, D. Maiolo, E. Carretti, P. Metrangolo, Halogen bonding modulates hydrogel formation from Fmoc amino acids, CrstEngComm. 19 (2017) 1870–1874, https://doi.org/10.1039/ C7CF00031F
- [25] M.J. Frisch G.W. Trucks H.B. Schlegel G.E. Scuseria M.a. Robb J.R. Cheeseman G. Scalmani V. Barone G.a. Petersson H. Nakatsuji X. Li M. Caricato a.V. Marenich J. Bloino B.G. Janesko R. Gomperts B. Mennucci H.P. Hratchian J.V. Ortiz a. F. Izmaylov J.L. Sonnenberg Williams F. Ding F. Lipparini F. Egidi J. Goings B. Peng A. PetroneT. Henderson D. Ranasinghe V.G. Zakrzewski J. Gao N. Rega G. Zheng W. Liang M. Hada M. Ehara K. Toyota R. Fukuda J. Hasegawa M. Ishida T. Nakajima Y. Honda O. Kitao H. Nakai T. Vreven K. Throssell J. a. Montgomery Jr. J.E. Peralta F. Ogliaro M.J. Bearpark J.J. Heyd E.N. Brothers K.N. Kudin V.N. Staroverov T. a. Keith R. Kobayashi J. Normand K. Raghavachari a. P. Rendell J.C. Burant S.S. Iyengar J. Tomasi M. Cossi J.M. Millam M. Klene C. Adamo R. Cammi J. W. Ochterski R.L. Martin K. Morokuma O. Farkas J.B. Foresman D.J. Fox G16_C01 2016 Gaussian 16 Revision A.03 Gaussian Inc., Wallin.
- [26] R. Krishnan, J.S. Binkley, R. Seeger, J.A. Pople, Self-consistent molecular orbital methods. XX. A basis set for correlated wave functions, J. Chem. Phys. 72 (1980) 650–654, https://doi.org/10.1063/1.438955.
- [27] A.D. Becke, A new mixing of hartree-fock and local density-functional theories, J. Chem. Phys. 98 (1993) 1372–1377, https://doi.org/10.1063/1.464304.
- [28] X. He, V.H. Man, W. Yang, T.-S. Lee, J. Wang, A fast and high-quality charge model for the next generation general AMBER force field, J. Chem. Phys. 153 (2020) 114502.
- [29] T. Lu, F. Chen, Multiwfn: A multifunctional wavefunction analyzer, J. Comput. Chem. 33 (2012) 580–592, https://doi.org/10.1002/jcc.22885.
- [30] T.J. Dolinsky, P. Czodrowski, H. Li, J.E. Nielsen, J.H. Jensen, G. Klebe, N.A. Baker, PDB2PQR: Expanding and upgrading automated preparation of biomolecular structures for molecular simulations, Nucleic Acids Res. 35 (2007) W522–W525, https://doi.org/10.1093/nar/gkm276.
- [31] M.J. Abraham, T. Murtola, R. Schulz, S. Páll, J.C. Smith, B. Hess, E. Lindahl, GROMACS: High performance molecular simulations through multi-level parallelism from laptops to supercomputers, SoftwareX. 1–2 (2015) 19–25, https://doi.org/10.1016/j.softx.2015.06.001.
- [32] H.J.C. Berendsen, J.P.M. Postma, W.F. van Gunsteren, A. DiNola, J.R. Haak, Molecular dynamics with coupling to an external bath, J. Chem. Phys. 81 (1984) 3684–3690, https://doi.org/10.1063/1.448118.
- [33] U. Essmann, L. Perera, M.L. Berkowitz, T. Darden, H. Lee, L.G. Pedersen, A smooth particle mesh Ewald method, J. Chem. Phys. 103 (1995) 8577–8593, https://doi. org/10.1063/1.470117.
- [34] J.N. Sloand, M.A. Miller, S.H. Medina, Fluorinated peptide biomaterials, Pept. Sci. 113 (2021) e24184.
- [35] S. Yuran, A. Dolid, M. Reches, Resisting bacteria and attracting cells: Spontaneous formation of a bifunctional peptide-based coating by on-surface assembly approach, ACS Biomater. Sci. Eng. 4 (2018) 4051–4061, https://doi.org/10.1021/ acsbiomaterials.8b00885.
- [36] T. Hu, M. Kaganovich, Z. Shpilt, A. Pramanik, O. Agazani, S. Pan, E. Tshuva, M. Reches, Ultrashort peptides for the self-assembly of an antiviral coating, Adv. Mater. Interfaces. 10 (2023) 2202161, https://doi.org/10.1002/admi.202202161.
- [37] M. Gupta, A. Bagaria, A. Mishra, P. Mathur, A. Basu, S. Ramakumar, V.S. Chauhan, Self-assembly of a dipeptide- containing conformationally restricted dehydrophenylalanine residue to form ordered nanotubes, Adv. Mater. 19 (2007) 858–861, https://doi.org/10.1002/adma.200601774.
- [38] D.A. Tinker, E.A. Krebs, I.C. Feltham, S.K. Attah-Poku, V.S. Ananthanarayanan, Synthetic beta-turn peptides as substrates for a tyrosine protein kinase, J. Biol. Chem. 263 (1988) 5024–5026, https://doi.org/10.1016/S0021-9258(18)60671-4.
- [39] P.I. Haris, D. Chapman, The conformational analysis of peptides using fourier transform IR spectroscopy, Biopolymers. 37 (1995) 251–263, https://doi.org/ 10.1002/bip.360370404.
- [40] S. Yuran, Y. Razvag, M. Reches, Coassembly of aromatic dipeptides into biomolecular necklaces, ACS Nano. 6 (2012) 9559–9566, https://doi.org/ 10.1021/nn302983e.
- [41] Z. Zhao, H. Matsui, Accurate immobilization of antibody-functionalized peptide nanotubes on protein-patterned arrays by optimizing their ligand-receptor interactions, Small. 3 (2007) 1390–1393, https://doi.org/10.1002/ smll.200700006.
- [42] J. Ryu, C.B. Park, High-temperature self-assembly of peptides into vertically well-aligned nanowires by aniline vapor, Adv. Mater. 20 (2008) 3754–3758, https://doi.org/10.1002/adma.200800364.
- [43] P. Kumaraswamy, R. Lakshmanan, S. Sethuraman, U.M. Krishnan, Self-assembly of peptides: Influence of substrate, pH and medium on the formation of supramolecular assemblies, Soft Matter. 7 (2011) 2744–2754, https://doi.org/ 10.1039/C0SM00897D.
- [44] M.J. Kratochvil, Y. Tal-Gan, T. Yang, H.E. Blackwell, D.M. Lynn, Nanoporous superhydrophobic coatings that promote the extended release of water-labile

- quorum sensing inhibitors and enable long-term modulation of quorum sensing in Staphylococcus aureus, ACS Biomater. Sci. Eng. $1\ (2015)\ 1039-1049$.
- [45] U.I.M. Gerling, M. Salwiczek, C.D. Cadicamo, H. Erdbrink, C. Czekelius, S.L. Grage, P. Wadhwani, A.S. Ulrich, M. Behrends, G. Haufe, B. Koksch, Fluorinated amino acids in amyloid formation: a symphony of size, hydrophobicity and α-helix propensity, Chem. Sci. 5 (2014) 819–830, https://doi.org/10.1039/C3SC52932K.
- [46] M.A. Greenfield, J.R. Hoffman, M. Olvera de la Cruz, S.I. Stupp, Tunable mechanics of peptide nanofiber gels, Langmuir 26 (2010) 3641–3647.
- [47] T. Hu, Y. Xu, G. Xu, S. Pan, Sequence-selected C13-dipeptide self-assembled hydrogels for encapsulation of lemon essential oil with antibacterial activity, J. Agric. Food Chem. 70 (2022) 7148–7157, https://doi.org/10.1021/acs. iafr 2c02385
- [48] E.T. Pashuck, H. Cui, S.I. Stupp, Tuning supramolecular rigidity of peptide fibers through molecular structure, J. Am. Chem. Soc. 132 (2010) 6041–6046, https://doi.org/10.1021/ja908560n.
- [49] J.F. Smith, T.P.J. Knowles, C.M. Dobson, C.E. MacPhee, M.E. Welland, Characterization of the nanoscale properties of individual amyloid fibrils, Proc. Natl. Acad. Sci. 103 (2006) 15806–15811, https://doi.org/10.1073/ pnas.0604035103.

- [50] S.B. Smith, Y. Cui, C. Bustamante, Overstretching B-DNA: The elastic response of individual double-stranded and single-stranded DNA molecules, Sci. 80 (271) (1996) 795–799, https://doi.org/10.1126/science.271.5250.795.
- [51] L. Adler-Abramovich, N. Kol, I. Yanai, D. Barlam, R.Z. Shneck, E. Gazit, I. Rousso, Self-assembled organic nanostructures with metallic-like stiffness, Angew Chemie. 122 (2010) 10135–10138.
- [52] N. Kol, L. Adler-Abramovich, D. Barlam, R.Z. Shneck, E. Gazit, I. Rousso, Self-assembled peptide nanotubes are uniquely rigid bioinspired supramolecular structures, Nano Lett. 5 (2005) 1343–1346, https://doi.org/10.1021/nl0505896.
- [53] M. Reches, E. Gazit, Casting metal nanowires within discrete self-assembled peptide nanotubes, Sci. 80 (300) (2003) 625–627, https://doi.org/10.1126/ science.1082387.
- [54] K. Manoharan, S. Bhattacharya, Superhydrophobic surfaces review: Functional application, fabrication techniques and limitations, J. Micromanufacturing. 2 (2019) 59–78, https://doi.org/10.1177/2516598419836345.
- [55] H.-J. Lee, W.S. Choi, 2D and 3D bulk materials for environmental remediation: Air filtration and oil/water separation, Materials (basel). 13 (2020), https://doi.org/ 10.3390/ma13245714.
- [56] Z. Dong, M. Vuckovac, W. Cui, Q. Zhou, R.H.A. Ras, P.A. Levkin, 3D printing of superhydrophobic objects with bulk nanostructure, Adv. Mater. 33 (2021) 2106068, https://doi.org/10.1002/adma.202106068.